International Journal of Bifurcation and Chaos

CONTROLLER DESIGN AND ANALYSIS FOR A TWO-CELL DC-DC CONVERTER IN PRESENCE OF SATURATION

R. HAMZA*
Research unit ICOS, École Nationale d'Ingnieurs de Sfax, Sfax, Tunisia

M. FEKI†
Research unit ICOS, École Nationale d'Ingnieurs de Sfax, Sfax, Tunisia

N. DERBEL‡
Research unit ICOS, École Nationale d'Ingnieurs de Sfax, Sfax, Tunisia

B. G. M. ROBERT§
Laboratoire CReSTIC, Universit de Reims-Champagne-Ardenne, Reims, France

A. EL AROUDI¶
GAEI Research group, Departament d'Enginyeria Electrònica, Elèctrica i Automàtica, Universitat Rovira i Virgili, Tarragona, Spain

Received on Feb 24, 2010
Accepted on Jul 02, 2010

In this work, a zero static error proportional controller for a two-cell DC-DC buck converter is synthesized and analyzed. Under a traditional proportional control scheme, the system presents a constant error of the current supplying the output load. As the proportional feedback gain is increased, the average static error decreases. However, sub-harmonic oscillations and chaotic behavior emerge beyond successive bifurcations. To achieve zero current and zero voltage static error, we suggest a modification of the traditional proportional controller. By optimizing the feedback gain, the settling time is also decreased. Then, using nonlinear analysis and Lyapunov stability theory, we prove that zero static error is achieved even in presence of duty cycle saturation. Numerical simulations are presented to confirm our theoretical results.

Keywords: Multi-cell converter; Converter control; Duty cycle saturation; State space model; Lyapunov stability; Bifurcations, Chaos; Subharmonics

*Research unit ICOS, École Nationale d'Ingnieurs de Sfax, Sfax, Tunisia
†Research unit ICOS, École Nationale d'Ingnieurs de Sfax, Sfax, Tunisia
‡Research unit ICOS, École Nationale d'Ingnieurs de Sfax, Sfax, Tunisia
§Laboratoire CReSTIC, Universit de Reims-Champagne-Ardenne, Reims, France
¶Author for correspondence: e-mail: abdelali.elaroudi@urv.cat

1. Introduction

During the last two decades, analysis, characterization and modeling of switching converters have been actively pursued [Deane & Hamill, 1992], [Tse, 1994], [Fossas & Olivar, 1996], [El Aroudi *et al.*, 2005], [Zhusubaliyev *et al.*, 2001, 2006]. Despite their simplicity, power converters have been shown to be copious in nonlinear dynamics [Huang & Tse, 2009; Nagy, 2000; Banerjee & Verghese, 2001]. Indeed, different types of bifurcations have been perceived in all their simple types: buck, buck-boost and boost converters [El Aroudi *et al.*, 2005], [di Bernardo & Tse, 2002], [Tse & di Bernardo, 2002]. A part from the standard singularities like period doubling and Hopf bifurcations, anomalous phenomena such as border collision bifurcations may also occur in these switched systems due to their nonsmoothness [Zhusubaliyev *et al.*, 2001, 2006]. These bifurcations are characterized by an abrupt jump in the eigenvalues of the Jacobian matrix of the map at a fixed point. Feigin was the first to develop a theory in the seventies for analyzing border collision bifurcations in such systems [Feigin , 1977]. The same class of systems was studied in [Nusse, 1994]. A classification of the types of bifurcations that can occur in piecewise smooth system was done in [di Bernardo *et al.*, 1999] and [Banerjee & Grebogi, 1999]. The theory for analyzing border-collision bifurcations in piecewise smooth systems is an active research topic and it was successfully applied to explain the strange behavior that can occur in DC-DC converters [Zhusubaliyev *et al.*, 2001] and in DC-AC inverters [Robert & Robert, 2002], [Wang *et al*, 2009].

Nonlinear behavior such as bifurcations and chaos occur in this kind of systems because of toggling between a set of linear or nonlinear circuit topologies under the action of a feedback control system and pulse width modulation. Border collision bifurcations occur because of the saturation of the duty cycles. Therefore, the control method as well as the circuit topology directly influence the dynamical behavior of the power converter [El Aroudi *et al.*, 2005].

In the last few years, there has been an interest in analyzing the nonlinear behavior of multi-cell power electronic converters [Robert & El Aroudi , 2006], [El Aroudi *et al.*, 2008]. These systems have been widely used in real applications since they circumvent shortcomings of ordinary switching devices due to their ability to support high-voltages [Tolbert & Peng, 2000]. Multi-cell converters applications include speed variation for medium and high voltage motors, voltage dynamic restoration and harmonics filtering. They have been also proposed for efficient wide-bandwidth envelope tracking in radio frequency power amplifiers [Yousefzadeh, 2005].

With appropriate control strategy, it was demonstrated that multi-cell power electronic converters can have exceptional performances in transients and in steady state. The goal of the control is to balance the flying capacitor voltage to a fraction of the input and to adjust the current to a reference level [Meynard *et al.*, 1997; Pirog *et al.* , 2006]. This is achieved by controlling the time durations during which the switches are conducting. Nevertheless, it has been shown that multi-cell DC-DC converters may also exhibit sub-harmonic modes and also chaotic behavior [Robert & El Aroudi , 2006]. As a matter of fact, the chaotic behavior usually emerges from bad tuning of the proportional gain while trying to increase it seeking least static error for the controlled variables. With the purpose of avoiding the chaotic behavior in this system and maintaining stable periodic regime, researchers tried to apply some techniques for controlling chaos. Recently a control technique called Fixed Point Induced Control (FPIC) was successfully applied to the elementary DC-DC two-cell DC-DC buck converter [El Aroudi *et al.*, 2009]. Basically, this technique is derived by compressing the Jacobian matrix of the closed loop system in such a way that with the modified control scheme, the eigenvalues of the system lie within the unit circle and therefore unstable periodic orbits are stabilized and possible chaotic and sub-harmonic oscillations are eliminated while the static error is reduced. Optimization of the dynamics of the system were carried out by studying these eigenvalues and minimizing their norms. However, saturation of duty cycles during start-up were completely ignored in the analysis.

This paper contains a generalization of the work presented in [Feki *et al.* , 2008]. Herein, we analyze the behavior of a proportional controller with different voltage gains and then a zero static error control technique is deduced and analyzed for a two-cell buck converter. The main interest of this study lies in the consideration of natural saturation of duty cycles, giving results about the response speed of the system taking into account practical aspects. As it will be shown later, the proposed technique is a powerful

strategy for avoiding sub-harmonic oscillations and chaotic behavior while eliminating the static error even in the presence of duty cycle saturation.

The rest of the paper is organized as follows: in Sec. 2, the system discrete-time model is derived. In Sec. 3, the analysis of the system behavior under a traditional proportional controller is presented. Some numerical simulation confirming the theoretical predictions are shown in the same section. In Sec. 4, the zero static error proportional controller is presented and its performances are studied analytically and by means of computer simulations. Then, in Sec. 5, a complete stability analysis taking into account saturating effect is presented. Finally, in the last section, some concluding remarks on this work are summarized.

2. Discrete-time Model of a Two-Cell Converter

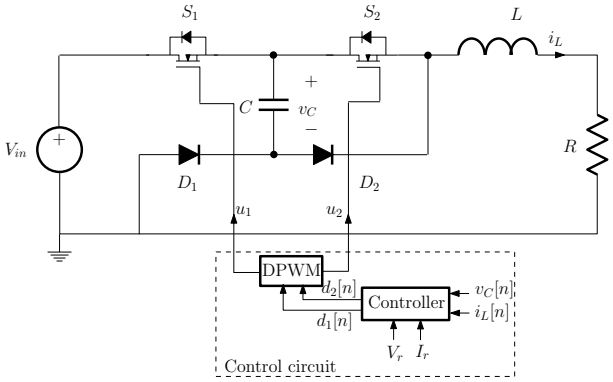

Fig. 1. A basic two-cell DC-DC buck converter.

The converter that we will deal with in this paper is depicted in Fig.1. It is based on a buck chopper modified in order to allow a higher input voltage by using two serial switches (transistors and diodes). The role of the capacitor is to balance the switch voltages. u_1 and u_2 are the outputs of a digital pulse width modulator (DPWM) driven by a feedback to be designed to achieve a constant voltage $v_C = \frac{V_{in}}{2}$ and a constant output current $i_L = I_r$, I_r being the reference current. It is worth noting here that if $v_C = \frac{V_{in}}{2}$, the total stress is shared between both switches making this structure suitable for high voltage applications. The controller is designed to define the duty cycles d_1 and d_2 of control voltages u_1 and u_2. The duty ratio is defined as the fraction of the switching period T during which the switch S_k is open that is in the OFF state. Thus, the switch S_k will remain in its OFF state during d_kT when it is driven by a control signal $u_k(t)$ with a duty cycle d_k. We assume here that the control voltages $u_1(t)$ and $u_2(t)$ are phase shifted by π in order to obtain optimum waveforms for the inductor current. That is the inductor current frequency is twice the switching frequency in this case [Meynard *et al.*, 1997].

In a typical operating mode the switch S_k and the diode D_k switch in a cyclic and periodic manner under the action of a fixed frequency digital pulse width modulator (DPWM). When the switch S_k is closed the diode D_k is open and vice versa. As we have two switches S_1 and S_2, then we can easily define four different operating topologies, (see Table 1). By applying Kirchhoff laws to the two-cell converter, the

Topologies	state of S_1	state of S_2
Topology 1 ($\mathcal{T}_1$)	OFF	ON
Topology 2 ($\mathcal{T}_2$)	ON	ON
Topology 3 ($\mathcal{T}_3$)	ON	OFF
Topology 4 ($\mathcal{T}_4$)	OFF	OFF

following switched model is obtained:

$$\frac{d}{dt}\begin{pmatrix} i_L \\ v_C \end{pmatrix} = \begin{pmatrix} -\frac{R}{L} & (u_2-u_1)\frac{1}{L} \\ (u_1-u_2)\frac{1}{C} & 0 \end{pmatrix}\begin{pmatrix} i_L \\ v_C \end{pmatrix} + \begin{pmatrix} \frac{V_{in}}{L}u_1 \\ 0 \end{pmatrix} \tag{1}$$

where u_k are the control signals for the switches S_k given by:

$$u_k = \begin{cases} 1 & \text{if} \quad S_k \quad \text{is closed (ON)} \\ 0 & \text{if} \quad S_k \quad \text{is open (OFF)} \end{cases} \tag{2}$$

Clearly, when u_1 and u_2 are replaced by 1 or 0, we obtain a linear system for each topology. Consequently, we can obtain analytic solution for each different topology. This fact is crucial for obtaining a discrete-time model of the two-cell converter.

2.1. *Obtaining the discrete-time model*

Toggling between different topologies occurs according to the values of the duty cycles d_1 and d_2 at the beginning of the period. As a matter of fact, we can define six different toggling modes (Fig.2), to each of which we can assign a recurrent map to express the values of the states at the end of the period in terms of the values at the beginning of the same PWM period T.

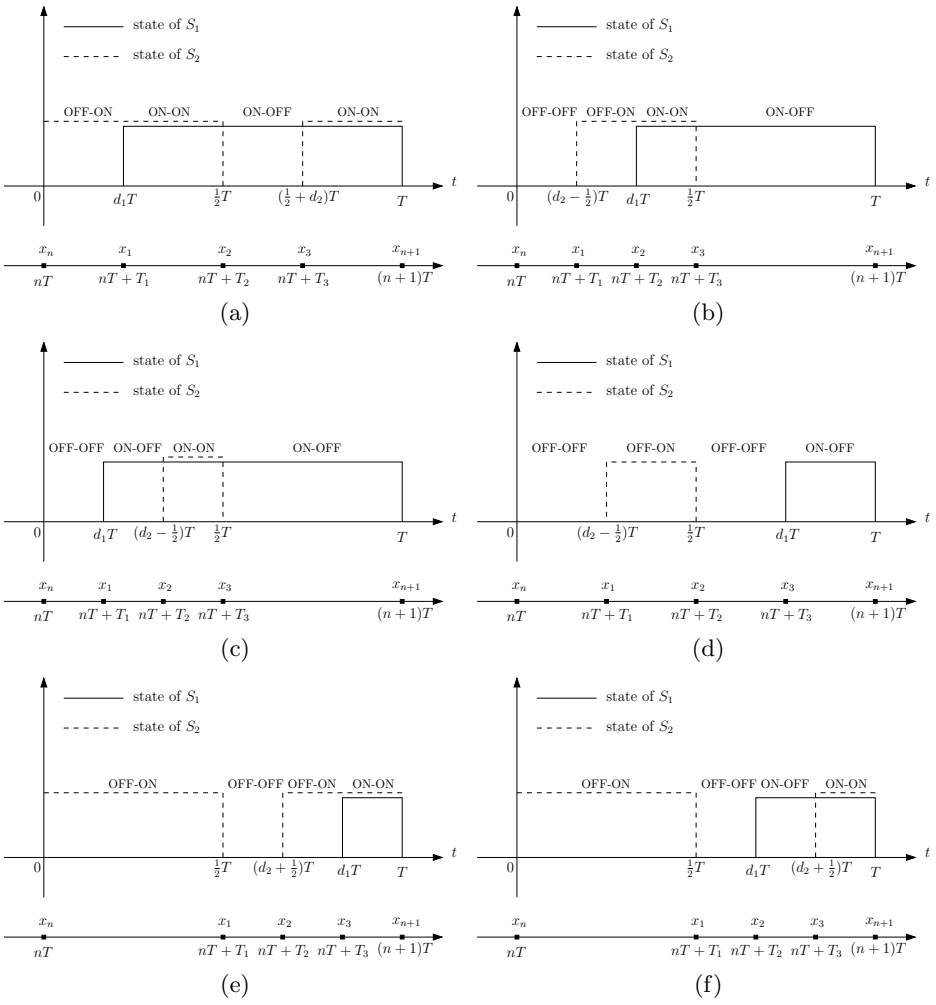

Fig. 2. Different possible operating modes for the two-cell DC-DC buck converter. (a) Mode 1: $d_1 < \frac{1}{2}$ and $d_2 < \frac{1}{2}$, (b) Mode 2: $d_1 < \frac{1}{2}$ and $0 < d_2 - \frac{1}{2} < d_1$, (c) Mode 3: $d_1 < \frac{1}{2}$ and $d_1 < d_2 - \frac{1}{2} < \frac{1}{2}$, (d) Mode 4: $d_1 > \frac{1}{2}$ and $d_2 > \frac{1}{2}$, (e) Mode 5: $d_1 > \frac{1}{2}$ and $\frac{1}{2} < d_2 + \frac{1}{2} < d_1$, (f) Mode 6: $d_1 > \frac{1}{2}$ and $\frac{1}{2} < d_1 < d_2 + \frac{1}{2} < 1$

Clearly, all modes divide the switching period into four interval and to each interval correspond a linear system so that during one switching period the two-cell converter can be described by the following piecewise linear switched model

$$\begin{array}{l} \dot{x} = A_1 x + B_1 \text{ during } \quad [nT, nT + t_1] \\ \dot{x} = A_2 x + B_2 \text{ during } [nT + t_1, nT + t_2] \\ \dot{x} = A_3 x + B_3 \text{ during } [nT + t_2, nT + t_3] \\ \dot{x} = A_4 x + B_4 \text{ during } [nT + t_3, (n+1)T] \end{array} \tag{3}$$

where A_k and B_k can be easily deduced from the switched model (1). The switching instants t_1, t_2 and t_3 are defined by the controller and the operating mode. The recurrent map of the specified mode is obtained by getting the analytic solutions and stacking them up. Six different recurrent maps are obtained. Because their expressions hold much space and they cannot be handled for theoretical analysis, they are not included in this paper. However, some results will be given in Sec. 4 for the sake of comparison between the exact model and the simplified one. Fortunately, the simplification of each recurrent model using practical assumptions[1] yielded to a unique model given by:

$$\begin{pmatrix} i_L[n+1] \\ v_C[n+1] \end{pmatrix} = \begin{pmatrix} 1 - \frac{TR}{L} & (d_1[n] - d_2[n])\frac{T}{L} \\ (d_2[n] - d_1[n])\frac{T}{C} & 1 \end{pmatrix} \begin{pmatrix} i_L[n] \\ v_C[n] \end{pmatrix} + \begin{pmatrix} \frac{V_{in}T}{L}(1 - d_1[n]) \\ 0 \end{pmatrix} \tag{4}$$

For the sake of reducing the number of parameters of the system we will consider some new dimensionless variables, where the current is scaled by the maximum output current, the voltage is scaled by the input voltage and time is normalized by the switching period. Let us consider the following changes of parameters and variables:

Parameters:

$$\delta_L = \frac{RT}{L}, \ \ \delta_C = \frac{T}{RC} \quad \text{and}$$

Variables:

$$x_i[n] = \frac{R i_L[n]}{V_{in}}, \ \ x_v[n] = \frac{v_C[n]}{V_{in}}$$

Therefore, we obtain the following dimensionless model:

$$\begin{pmatrix} x_i[n+1] \\ x_v[n+1] \end{pmatrix} = \begin{pmatrix} 1 - \delta_L & (d_1[n] - d_2[n])\delta_L \\ (d_2[n] - d_1[n])\delta_C & 1 \end{pmatrix} \begin{pmatrix} x_i[n] \\ x_v[n] \end{pmatrix} + \begin{pmatrix} \delta_L(1 - d_1[n]) \\ 0 \end{pmatrix} \tag{5}$$

In order to reduce the current ripple through the load and the voltage ripple across the capacitor, the circuit parameters should satisfy $\delta_L \ll 1$ and $\delta_C \ll 1$. In the sequel, simulations will be carried out with the following parameters:

$$\delta_L = 0.1, \quad \delta_C = 0.1, \quad I_r = 0.6 \ \text{ and } \ V_r = 0.5$$

3. Converter Behavior Under Traditional Proportional Controller Action

Before to proceed any further, we notice that the recurrent model (5) can be described as a generalized bilinear model. Indeed, we have:

$$x[n+1] = \mathbb{A}_0 x[n] + \mathbb{A}_1 x[n]\mu_1[n] + \mathbb{B}\mu_2[n] \tag{6}$$

where

$$\mathbb{A}_0 = \begin{pmatrix} 1 - \delta_L & 0 \\ 0 & 1 \end{pmatrix}, \quad \mathbb{A}_1 = \begin{pmatrix} 0 & \delta_L \\ -\delta_C & 0 \end{pmatrix}, \quad \mathbb{B} = \begin{pmatrix} \delta_L \\ 0 \end{pmatrix},$$

[1]The current and voltage time constants are much larger than the switching period so that these state variables are considered straight lines during each switching interval.

$$\mu_1[n] = d_1[n] - d_2[n] \ , \quad \text{and} \quad \mu_2[n] = 1 - d_1[n]$$

We can easily verify that the pair $(\mathbb{A}_0, \mathbb{B})$ is not controllable whereas the pair $(\mathbb{A}_1, \mathbb{B})$ is controllable. Thus if $d_1[n] = d_2[n]$ then the voltage state variable is not controllable but we notice that the eigenvalues of $\mathbb{A}_0$, namely $(1 - \delta_L, 1)$, are within the unit circle. Thus, in that case the two-cell converter has a critically stable fixed point $(x_i^*, x_v^*) = (1 - d_1^*, x_v[0])$, where d_1^* is evaluated at the fixed point. Eventually, we deduce that any successful control strategy should either lead to $d_1[n] \neq d_2[n]$ or at least $d_1[n] = d_2[n]$ only if $x_v[n] = V_r$. In this section, we present an analysis and numerical simulations when the converter is under the action of a traditional proportional controller. Herein, the duty cycles are made different by the choice of different voltage proportional gains k_{v1} and k_{v2}:

$$d_1[n] = k_i(x_i[n] - I_r) + k_{v1}(x_v[n] - V_r) \tag{7}$$
$$d_2[n] = k_i(x_i[n] - I_r) + k_{v2}(x_v[n] - V_r) \tag{8}$$

where k_i is the proportional current gain. We implicitly understand from any expression of the duty cycles d_1 and d_2 that they undergo a saturation because they neither can be negative, nor greater than one because the OFF state can not be larger than the switching period. Therefore, the applied duty cycle is in fact $\text{sat}(d_k)$ and not d_k, where $\text{sat}(d)$ is the function defined by:

$$\text{sat}(d) = \frac{1}{2}\left(1 + |d| - |d - 1|\right) \tag{9}$$

The aim of the proportional controller is to drive the states $x_i[n]$ to I_r and $x_v[n]$ to V_r. Hence, by defining $e_i[n] = x_i[n] - I_r$ and $e_v[n] = x_v[n] - V_r$, the aim becomes to drive the error variables to zero. To accomplish this aim, we need first to describe the error dynamics. Indeed, by simple algebra, we obtain:

$$\begin{pmatrix} e_i[n+1] \\ e_v[n+1] \end{pmatrix} = \begin{pmatrix} 1 - \delta_L & 0 \\ 0 & 1 \end{pmatrix} \begin{pmatrix} e_i[n] \\ e_v[n] \end{pmatrix} + \begin{pmatrix} (d_1 - d_2)\delta_L x_v[n] \\ (d_2 - d_1)\delta_C x_i[n] \end{pmatrix} + \begin{pmatrix} -\delta_L d_1 + \delta_L(1 - I_r) \\ 0 \end{pmatrix} . \tag{10}$$

This is a non-autonomous system due to the presence of the independent signals $x_i[n]$ and $x_v[n]$ and the constant term $\delta_L(1 - I_r)$. By applying the proportional controller we get the following error dynamics

$$\begin{pmatrix} e_i[n+1] \\ e_v[n+1] \end{pmatrix} = \begin{pmatrix} 1 - \delta_L(k_i + 1) & (k_{v1} - k_{v2})\delta_L x_v[n] - \delta_L k_{v1}) \\ 0 & 1 - (k_{v1} - k_{v2})\delta_C x_i[n] \end{pmatrix} \begin{pmatrix} e_i[n] \\ e_v[n] \end{pmatrix} + \begin{pmatrix} \delta_L(1 - I_r) \\ 0 \end{pmatrix} \tag{11}$$

Assuming that $k_{v1} \neq k_{v2}$ and $x_i[n] > 0$, the fixed point of the system is $(e_i^*, e_v^*) = \left(\frac{1 - I_r}{1 + k_i}, 0\right)$. Since the obtained error system is non-autonomous, then we will determine its stability conditions using Lyapunov theory. First, note that the error dynamics in (11) can be written in general under the triangular form:

$$e_v[n+1] = f_1(e_v[n]) \tag{12}$$
$$e_i[n+1] = f_2(e_v[n], e_i[n]) \tag{13}$$

It has been proved that under mild conditions (verified by system (11)), the asymptotic stability of system (12)-(13) can be deduced from the simultaneous asymptotic stability of the following subsystems [Bai *et al.*, 2006]:

$$e_v[n+1] = f_1(e_v[n]) \tag{14}$$
$$e_i[n+1] = f_2(e_v^*, e_i[n]) \tag{15}$$

where e_v^* is the equilibrium point of (14). Now, the first subsystem is described by:

$$e_v[n+1] = (1 - (k_{v1} - k_{v2})\delta_C x_i[n])e_v[n] \tag{16}$$

This is a first order non-autonomous system, so we may consider the Lyapunov function candidate $V(e_v[n]) = e_v[n]^2$. In discrete systems we need to show that the variation of the Lyapunov function is negative $\Delta V(e_v[n]) = V(e_v[n+1]) - V(e_v[n]) < 0$.

$$\Delta V(e_v[n]) = \Big((1 - (k_{v1} - k_{v2})\delta_C x_i[n])^2 - 1\Big)e_v[n]^2 \tag{17}$$
$$= (k_{v1} - k_{v2})\delta_C x_i[n]\Big((k_{v1} - k_{v2})\delta_C x_i[n] - 2\Big)e_v[n]^2 \tag{18}$$

Knowing that $x_i[n]$ is always positive, then we can guarantee that ΔV is negative if the voltage gains k_{v1} and k_{v2} are chosen to satisfy condition (19).

$$0 < k_{v1} - k_{v2} < \frac{2}{\delta_C x_i[n]} \tag{19}$$

We can also optimize the difference $\Delta k_v = k_{v1} - k_{v2}$ to obtain fast convergence of the voltage error to zero. This is done by minimizing $\Delta V(e_v[n])$, therefore we need to minimize the function

$$h(\Delta k_v) = \Delta k_v \delta_C x_i[n]\Big(\Delta k_v \delta_C x_i[n] - 2\Big) \tag{20}$$

with respect to Δk_v and we get

$$\left.\frac{dh}{d\Delta k_v}\right|_{\Delta k_v = \Delta k_{v,opt}} = 0 \tag{21}$$

which implies:

$$\Delta k_{v,opt} \delta_C x_i[n] - 1 = 0 \tag{22}$$

and therefore the optimum difference between k_{v1} and k_{v2} is

$$\Delta k_{v,opt} = \frac{1}{\delta_C x_i[n]} \tag{23}$$

Until now, we can guarantee the stability of subsystem (16) at the origin by the choice of Δk_v. Next, we will investigate the stability of the second subsystem:

$$\begin{aligned} e_i[n+1] &= f_2(0, e_i[n]) \\ &= \big(1 - \delta_L(1+k_i)\big)e_i[n] + \delta_L(1 - I_r) \end{aligned} \tag{24}$$

Clearly, the fixed point of the second subsystem is not zero but $e_i^* = \frac{1-I_r}{1+k_i}$. Thus, using a new variable $\epsilon_i[n] = e_i[n] - e_i^*$, we obtain:

$$\epsilon_i[n+1] = \big(1 - \delta_L(1+k_i)\big)\epsilon_i[n] \tag{25}$$

This is a linear first order system that will be stable if the current gain satisfies:

$$-1 < k_i < \frac{2}{\delta_L} - 1 = k_{i,cri} \tag{26}$$

Although, the lower value of k_i in (26) is -1, this lower boundary must be positive to avoid saturation of the duty cycle at steady state. To obtain fast convergence, the eigenvalue corresponding to this state variable should be placed at the origin and therefore the current gain should be fixed to:

$$k_{i,opt} = \frac{1}{\delta_L} - 1 \tag{27}$$

On the other hand, to obtain zero current error $e_i^* = \frac{1-I_r}{1+k_i}$, k_i should be raised to infinity. Thus, by using a traditional proportional controller, the current reference I_r can not be achieved and the minimum error that can be reached is with $k_i \to k_{i,cri}$:

$$e_{i,\min} > \delta_L \frac{1 - I_r}{2} \tag{28}$$

In Fig.3, we present the response of the two-cell converter under the action of a traditional proportional controller.

Remark 3.1. We notice that the stability condition given in (19) constraints the difference between k_{v1} and k_{v2}. Nevertheless, this does not mean that any values of the voltage gains satisfying (19) will be suitable for the proportional controller to attend the fixed point $(e_i^*, e_v^*) = \big(\frac{1-I_r}{1+k_i}, 0\big)$ or equivalently $(x_i^*, x_v^*) = \big(\frac{1+k_i I_r}{1+k_i}, V_r\big)$. In fact, one should be careful not to choose values of k_{v1} and k_{v2} that lead to saturation of $d_1[n]$ and $d_2[n]$ on the same side. The result of that action will be having an uncontrollable state $x_v[n]$.

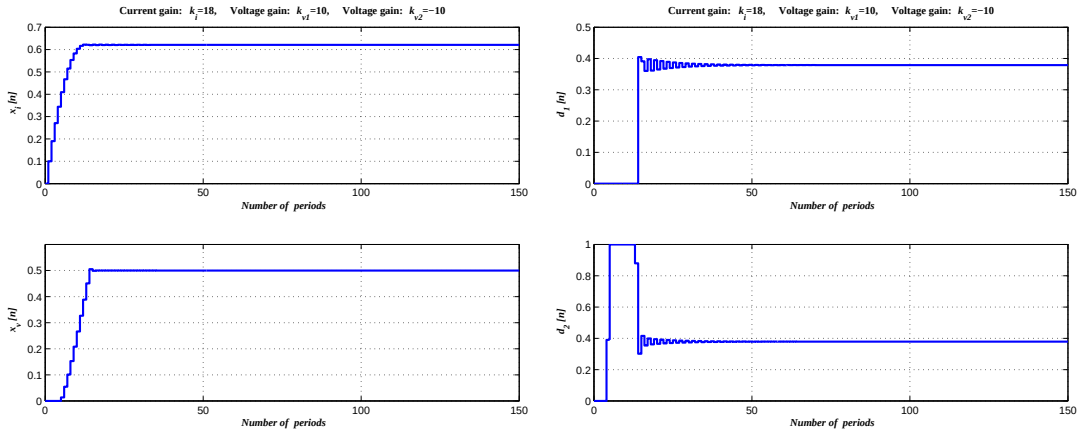

(a) (b)

Fig. 3. Response of the two-cell converter under the action of a traditional proportional controller. (a) Time evolution of the state variables $x_i[n]$ and $x_v[n]$, (b) Time evolution of the duty cycles $d_1[n]$ and $d_2[n]$.

Actually, the present analysis does not take into account the saturation phenomenon. However, when k_{v1} and k_{v2} are chosen to satisfy (19) but according to the initial conditions, both duty cycles saturate on the same side, then we get $d_1[n] = d_2[n]$ and we get an uncontrollable voltage state variable that is the initial voltage is maintained throughout the saturation duration. Whereas the current will reach a constant value either $x_i[n] = 1$ when saturation of the duty cycles occurs at $d_1[n] = d_2[n] = 0$ or $x_i[n] = 0$ when saturation of the duty cycles occurs at $d_1[n] = d_2[n] = 1$. For instance, if we consider the practical case of a starting procedure $x_v[0] = 0$ and $x_i[0] = 0$, then if $k_{v2} < k_{v1} < \frac{1-k_i e_i[0]}{e_v[0]}$ then both duty cycles saturate at one, $d_1[n] = d_2[n] = 1$. In this case, we get a stable fixed point of (5) at $(x_i^*, x_v^*) = (0, x_{v,0})$ as depicted in Fig.4. However, if $k_{v1} > k_{v2} > -\frac{k_i e_i[0]}{e_v[0]}$ is satisfied, we obtain saturated duty cycles $d_1[n] = d_2[n] = 0$, then $x_i[n]$ tends to 1 and there may not be saturation and the fixed point $(x_i^*, x_v^*) = \left(\frac{1+k_i I_r}{1+k_i}, V_r\right)$ will be achieved. Should $k_{v1} > k_{v2} > -\frac{k_i(1-I_r)}{e_v[0]}$ be satisfied then we obtain saturated duty cycles $d_1[n] = d_2[n] = 0$ for all current values $x_i[n]$. In this case, we get a stable fixed point of (5) at $(x_i^*, x_v^*) = (1, x_v[0])$ as depicted in Fig.5.

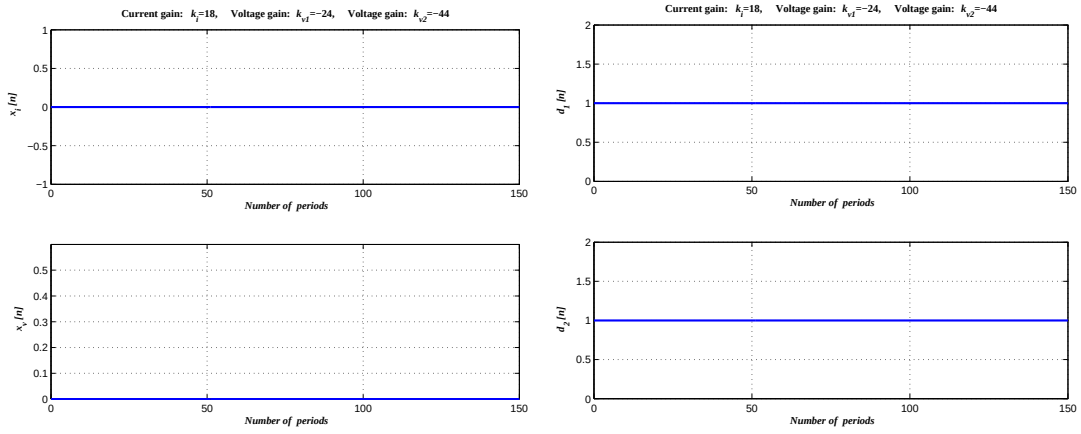

(a) (b)

Fig. 4. Response of the two-cell converter under the action of a proportional controller with voltage gains yielding to duty cycles saturation $d_1[n] = d_2[n] = 1$. (a) Time evolution of the state variables $x_i[n]$ and $x_v[n]$, (b) Time evolution of the duty cycles $d_1[n]$ and $d_2[n]$.

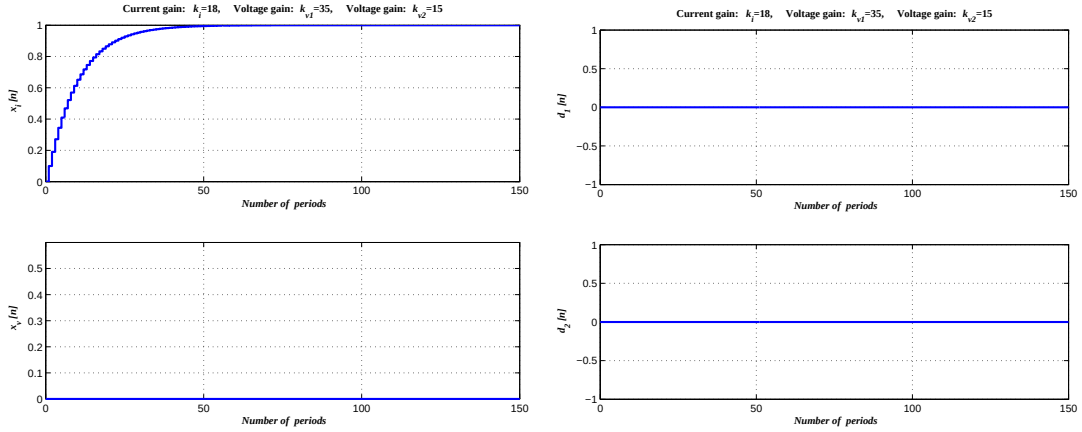

(a) (b)

Fig. 5. Response of the two-cell converter under the action of a proportional controller with voltage gains yielding to duty cycles saturation $d_1[n] = d_2[n] = 0$. (a) Time evolution of the state variables $x_i[n]$ and $x_v[n]$, (b) Time evolution of the duty cycles $d_1[n]$ and $d_2[n]$.

Figures 6 and 7 depict simulation results where initial condition leads to saturation at zero but when $x_i[n]$ increases to 1 saturation vanishes. The proportional voltage gains k_{v1} and k_{v2} are pushed respectively towards their negative limit ($k_{v1} > k_{v2} \gtrsim -\frac{k_i e_i[0]}{e_v[0]}$) and positive limit ($-\frac{k_i(1-I_r)}{e_v[0]} \gtrsim k_{v1} > k_{v2}$) that lead to the fixed point $(x_i^*, x_v^*) = \left(\frac{1+k_i I_r}{1+k_i}, V_r\right)$. The time response is large and the convergence is very slow.

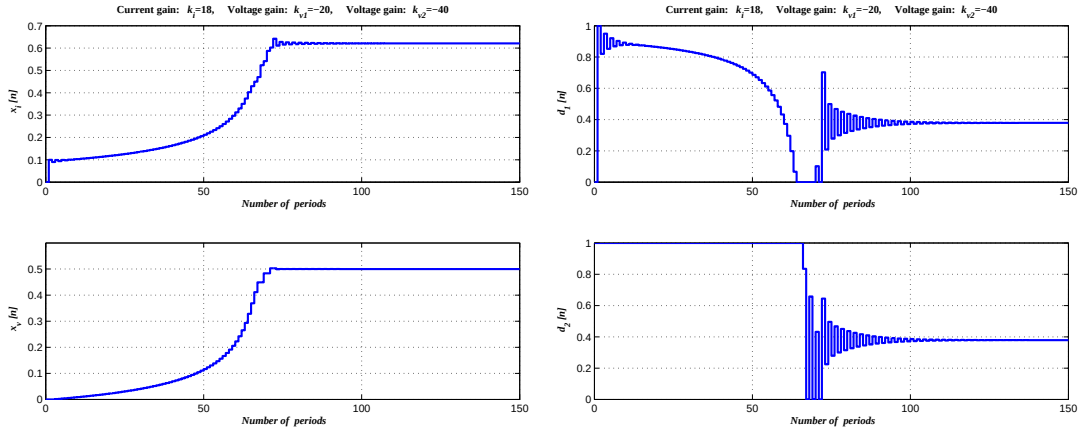

(a) (b)

Fig. 6. Response of the two-cell converter under the action of a proportional controller having negative voltage gains near limit of stability. (a) Time evolution of the state variables $x_i[n]$ and $x_v[n]$, (b) Time evolution of the duty cycles $d_1[n]$ and $d_2[n]$.

Figures 6 and 7 show simulation results where the proportional voltage gains k_{v1} and k_{v2} are pushed towards the lower and upper stability limit respectively yielding to large time response and very slow convergence to the normal fixed point. It is noticed that when the voltage gains are pushed out of the stability limits, saturation of the duty cycles occurs. In [Robert & El Aroudi , 2006], the authors proved that when the current gain is pushed out of the stability limits, then chaotic behavior is obtained. The chaotic behavior is well delineated using the bifurcation diagram of Fig.8. The voltage gains were fixed to $k_{v1} = -k_{v2} = 10$. The curves in red represent the current values at which the duty cycle saturates. Since at steady state we have $x_v[n] = V_r$ for all k_i, then (7) and (8) imply that $d_1[n] = d_2[n]$ and hence both duty cycles have similar upper and lower saturation limits. These limits occur when $d_k[n] = 1$ and when

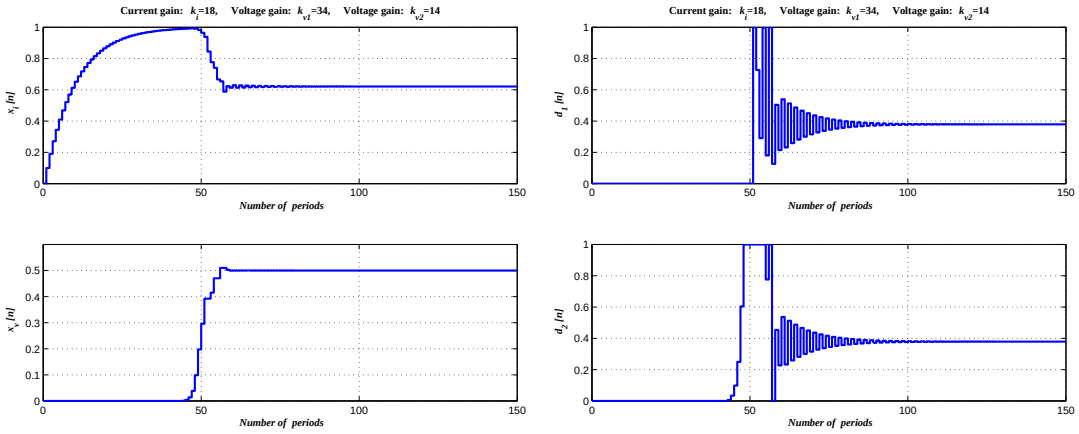

(a) (b)

Fig. 7. Response of the two-cell converter under the action of a proportional controller having positive voltage gains near limit of stability. (a) Time evolution of the state variables $x_i[n]$ and $x_v[n]$, (b) Time evolution of the duty cycles $d_1[n]$ and $d_2[n]$.

$d_k[n] = 0$ that is:

$$d_k[n] = 1 \Leftrightarrow x_{i,sat,upper} = \frac{1}{k_i} + I_r \tag{29}$$

$$d_k[n] = 0 \Leftrightarrow x_{i,sat,lower} = I_r \tag{30}$$

These limits are depicted in Fig. 8 in red color.

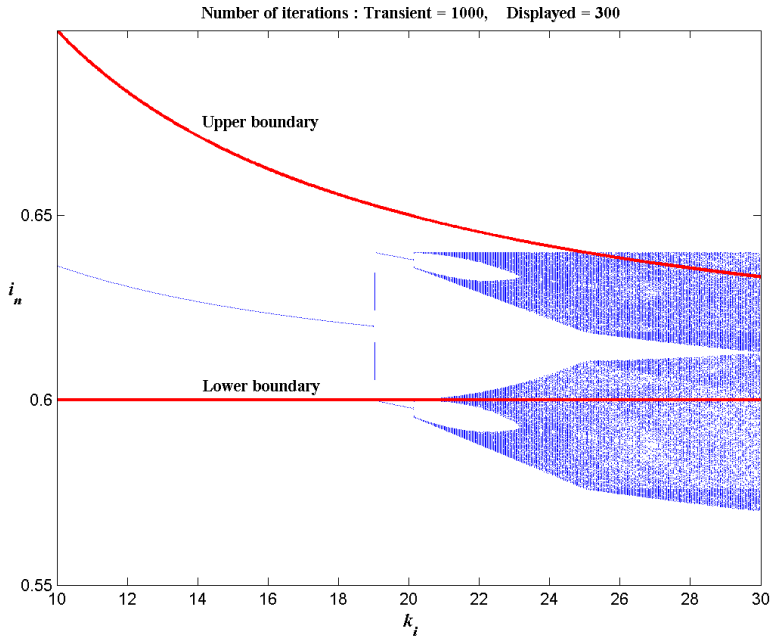

Fig. 8. Bifurcation diagram of the inductor current in the two-cell converter.

4. Zero Static Error Controller Design

When applying the proportional controller, we obtain zero voltage error $e_v[n] = 0$. According to (7) and (8), this makes $d_1[n] = d_2[n] = k_i e_i[n]$. Moreover, when the duty cycles are equal, the current tends to the fixed point $x_i^* = 1 - d_1^*$, so we have:

$$\lim_{n\to\infty} x_i[n] - (1 - d_1[n]) = 0 \tag{31}$$

Hence, we may obtain $\lim_{n\to\infty} x_i[n] = I_r$ only if

$$\lim_{n\to\infty} d_1[n] = 1 - I_r \ . \tag{32}$$

Besides, if $\lim_{n\to\infty} x_i[n] \neq 0$ and $\lim_{n\to\infty} x_v[n] \neq 0$, then from (11), we can get $\lim_{n\to\infty} e_i[n] = 0$ and $\lim_{n\to\infty} e_v[n] = 0$ only if $\lim_{n\to\infty} d_2[n] = \lim_{n\to\infty} d_1[n] = 1 - I_r$. If we choose $d_1 = d_2 = 1 - I_r$, then we are clearly left with a linear error dynamics:

$$\begin{pmatrix} e_i[n+1] \\ e_v[n+1] \end{pmatrix} = \begin{pmatrix} 1-\delta_L & 0 \\ 0 & 1 \end{pmatrix} \begin{pmatrix} e_i[n] \\ e_v[n] \end{pmatrix} \ , \tag{33}$$

which have a stable current state variable with $\lambda_i = (1 - \delta_L)$ and a critically stationary voltage state variable with $\lambda_v = 1$. This controller is an open loop type that leads to $\lim_{n\to\infty} x_i[n] = I_r$ but $x_v[n] = x_v[0]$ for all instants n. Therefore, we cannot attend our aim with this type of controller.

If we add to $1 - I_r$ a term proportional to the voltage error we obtain a controllable voltage mode. Indeed, by the application of the following duty cycles:

$$d_1[n] = 1 - I_r + k_{v1}(x_v[n] - V_r) \tag{34}$$

$$d_2[n] = 1 - I_r + k_{v2}(x_v[n] - V_r) \tag{35}$$

The closed loop system becomes:

$$\begin{pmatrix} e_i[n+1] \\ e_v[n+1] \end{pmatrix} = \begin{pmatrix} 1-\delta_L & (k_{v1}-k_{v2})\delta_L x_v[n] - \delta_L k_{v1}) \\ 0 & 1-(k_{v1}-k_{v2})\delta_C x_i[n] \end{pmatrix} \begin{pmatrix} e_i[n] \\ e_v[n] \end{pmatrix} \tag{36}$$

Here again, the system is in the triangular form (12)-(13), where the first subsystem is identical to (16). Therefore, similar conditions apply to the voltage gains; namely condition (19) for stability and (23) for optimality. However, for the second subsystem, we get:

$$e_i[n+1] = (1 - \delta_L)e_i[n] \tag{37}$$

which is a stable linear system to which we have no control on the convergence speed which is rather slow since $\delta_L \ll 1$. Figure 9 depicts the response of the two-cell converter under the action of controller (34)-(35) while respecting the optimality criterion (23). Although our aim of achieving the current and voltage references with zero static error was attained, we have very slow convergence of the current to its reference. The aim of this last suggestion is to force the current and the voltage to converge to the reference values as fast as possible. To achieve our aim we let

$$d_1[n] = 1 - I_r + k_i(x_i[n] - I_r) + k_{v1}(x_v[n] - V_r) \tag{38}$$

$$d_2[n] = 1 - I_r + k_i(x_i[n] - I_r) + k_{v2}(x_v[n] - V_r) \tag{39}$$

After application of (38)-(39), the closed loop system becomes:

$$\begin{pmatrix} e_i[n+1] \\ e_v[n+1] \end{pmatrix} = \begin{pmatrix} 1-\delta_L(1+k_i) & (k_{v1}-k_{v2})\delta_L x_v[n] - \delta_L k_{v1}) \\ 0 & 1-(k_{v1}-k_{v2})\delta_C x_i[n] \end{pmatrix} \begin{pmatrix} e_i[n] \\ e_v[n] \end{pmatrix} \tag{40}$$

Similar analysis to that carried out in the previous section ((23), (27)) shows that $\Delta k_{v,opt} = \frac{1}{\delta_C x_i[n]}$ and that $k_{i,opt} = \frac{1}{\delta_L} - 1$ but in this case we obtain zero static error. Again, one may badly choose the voltage gains while satisfying the optimality condition. Indeed, if $k_i = k_{i,opt} = 9$ and the voltage gains are chosen such that the duty cycles d_1 and d_2 saturate on the same side then we may not achieve $e_i = e_v = 0$. If we consider the practical case of $x_i[0] = 0$ and $x_v[0] = 0$, then we can distinguish several cases for

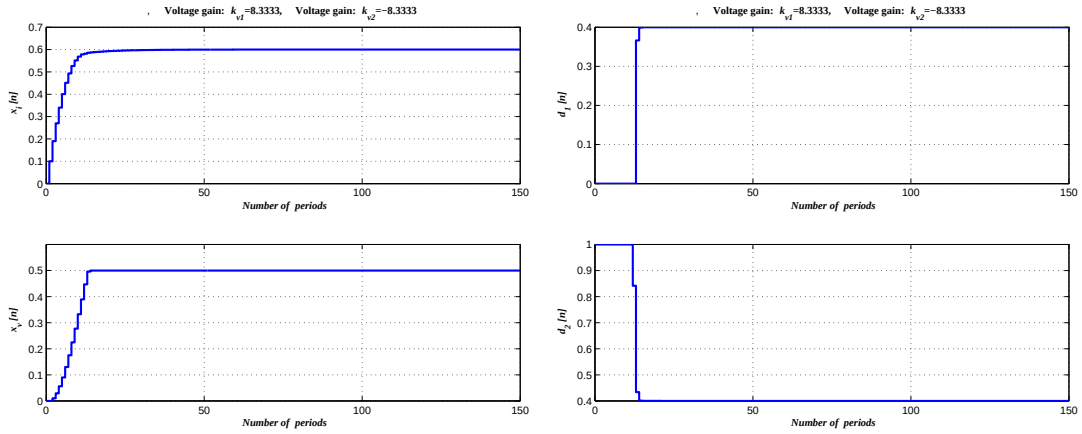

(a) (b)

Fig. 9. Response of the two-cell converter under the action of controller (34)-(35). (a) Time evolution of the state variables $x_i[n]$ and $x_v[n]$, (b) Time evolution of the duty cycles $d_1[n]$ and $d_2[n]$.

choices of k_{v1} and k_{v2}. Indeed, if $k_{v1} < \frac{I_r - k_i e_i[0]}{e_v[0]}$ and Δk_v satisfies the optimality condition, we obtain saturated duty cycles $d_1 = d_2 = 1$. In this case, the fixed point of (5) is $(x_i^*, x_v^*) = (0, x_v[0])$ and therefore for the chosen initial condition is stable. However, if $k_{v2} > -\frac{1 - I_r + k_i e_i[0]}{e_v[0]}$ and k_{v1} satisfies the optimality condition, we obtain saturated duty cycles $d_1 = d_2 = 0$. In this case, we get a stable fixed point of (5) at $(x_i^*, x_v^*) = (1, x_v[n])$. Thus, zero error static $e_i = e_v = 0$ will not be achieved. Figure 10 shows the response of the two-cell converter under the action of the controller (38)-(39) with optimum gains applied to system (5). The voltage dynamics is similar to those shown on Fig. 10. However, we notice that zero current static error was achieved within 14 periods only. In Fig.11 we show the effect of the same controller on the exact (non simplified) discrete-time model that lead to (5) after simplification. We notice that zero static errors have been also achieved but after 16 periods.

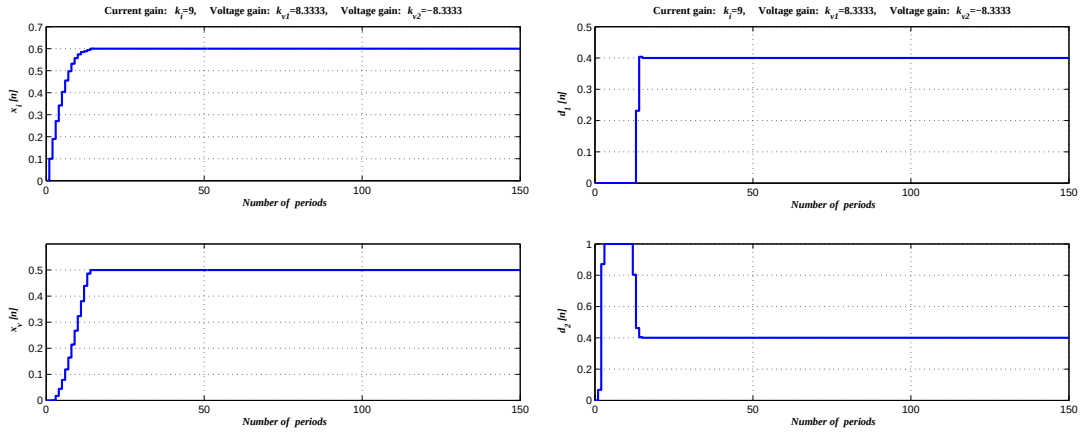

(a) (b)

Fig. 10. Response of the two-cell converter simplified model under the action of controller (38)-(39) with optimum gains. (a) Time evolution of the state variables $x_i[n]$ and $x_v[n]$, (b) Time evolution of the duty cycles $d_1[n]$ and $d_2[n]$.

5. Complete Stability Analysis: Saturation Effect

The stability analysis, presented in the previous sections, has not considered the evident saturation of the duty cycles except for the special cases where saturation occurs on the same side which hinders the controller

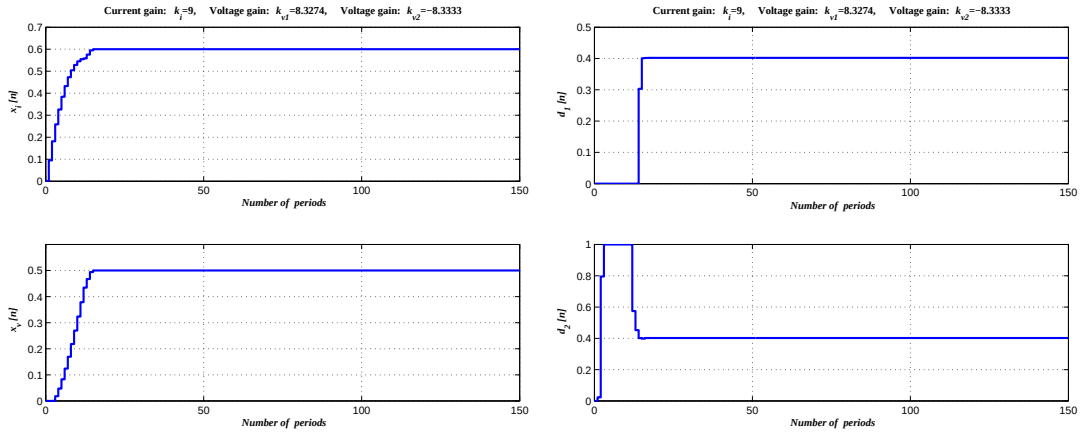

(a) (b)

Fig. 11. Response of the two-cell converter exact model under the action of controller (38)-(39) with optimum gains. (a) Time evolution of the state variables $x_i[n]$ and $x_v[n]$, (b) Time evolution of the duty cycles $d_1[n]$ and $d_2[n]$.

from reaching its aim. We have seen that this occurs when the two voltage gains lie simultaneously beyond a certain limit. To overcome these phenomena, we add a new constraint by choosing opposite voltage gains. Nevertheless, when looking at the duty cycles evolution for all different controllers that have been suggested in this paper, we notice that they inevitably saturate during the transient time. In spite of this fact, the stability analysis has not considered the saturation of the duty cycles, therefore, it is not reliable. In this section, we try to present a concrete proof to show that the two-cell converter is in fact stabilized with the proposed controller (38)-(39) even in the presence of duty cycle saturation. For simplicity of the demonstration, as mentioned above, the study is limited to the particular case where $k_{v1} = -k_{v2} = k_v$. To our knowledge, very few works in literature have considered the saturation phenomenon [Feki *et al.* , 2008]. Let $\mathcal{R}$ defines the space of all possible errors:

$$\mathcal{R} = \{(e_i[n], e_v[n]) | -I_r \leq e_i[n] \leq 1 - I_r, -V_r \leq e_v[n] \leq 1 - V_r\} \tag{41}$$

Clearly, the saturation of both duty cycles defines four boundaries in $\mathcal{R}$. These boundaries are in the form of lines defined by:

$$\mathcal{L}_{11}: \ d_1 = 1 \quad \Rightarrow \quad -I_r + k_i e_i[n] + k_v e_v[n] = 0 \tag{42}$$

$$\mathcal{L}_{10}: \ d_1 = 0 \quad \Rightarrow \quad 1 - I_r + k_i e_i[n] + k_v e_v[n] = 0 \tag{43}$$

$$\mathcal{L}_{21}: \ d_2 = 1 \quad \Rightarrow \quad -I_r + k_i e_i[n] - k_v e_v[n] = 0 \tag{44}$$

$$\mathcal{L}_{20}: \ d_2 = 0 \quad \Rightarrow \quad 1 - I_r + k_i e_i[n] - k_v e_v[n] = 0 \tag{45}$$

These boundary lines divide the error space into nine subspaces denoted by $\mathcal{R}_j$, such that $\bigcup_{j=1}^{j=9} \mathcal{R}_j = \mathcal{R}$ (see Fig. 12). In each subspace, the two-cell converter is described by a different model (denoted by $\mathcal{M}_j$) that can be obtained from (5) by replacing the duty cycles by their corresponding values, namely $d_k[n] = 0$ or $d_k[n] = 1$ or the expressions given in (38)-(39).

We now consider the following Lyapunov function:

$$V(e[n]) = e_i[n]^2 + e_v[n]^2 \tag{46}$$

Then, we can verify that $\Delta V = V(e[n+1]) - V(e[n]) < 0$ for each model $\mathcal{M}_j$ in the subspace $\mathcal{R}_j$ except at the origin where $\Delta V = 0$. For example, in region $\mathcal{R}_1$ we have:

$$\Delta V = \delta_L(\delta_L - 2)e_i[n]^2 + \delta_L I_r\big(\delta_L I_r - 2(1 - \delta_L)e_i[n]\big) \tag{47}$$

Taking into account that $\delta_L \ll 1$, it follows that $\Delta V < 0$ if $e_i[n] > \frac{\delta_L I_r}{2(1-\delta_L)}$. In addition, we know that if $k_{v2} < 0 < k_{v1}$ then $e_i[n] > \frac{I_r}{k_i}$ in region $\mathcal{R}_1$, thus it is sufficient to choose $k_i < \frac{2(1-\delta_L)}{\delta_L}$ to obtain $\Delta V < 0$. We notice that the obtained condition is satisfied by $k_{i,opt}$. In region $\mathcal{R}_2$ we may easily verify that:

$$\Delta V = \delta_L(\delta_L - 2)e_i[n]^2 + \delta_L(1 - I_r)\big(\delta_L(1 - I_r) + 2(1 - \delta_L)e_i[n]\big) \tag{48}$$

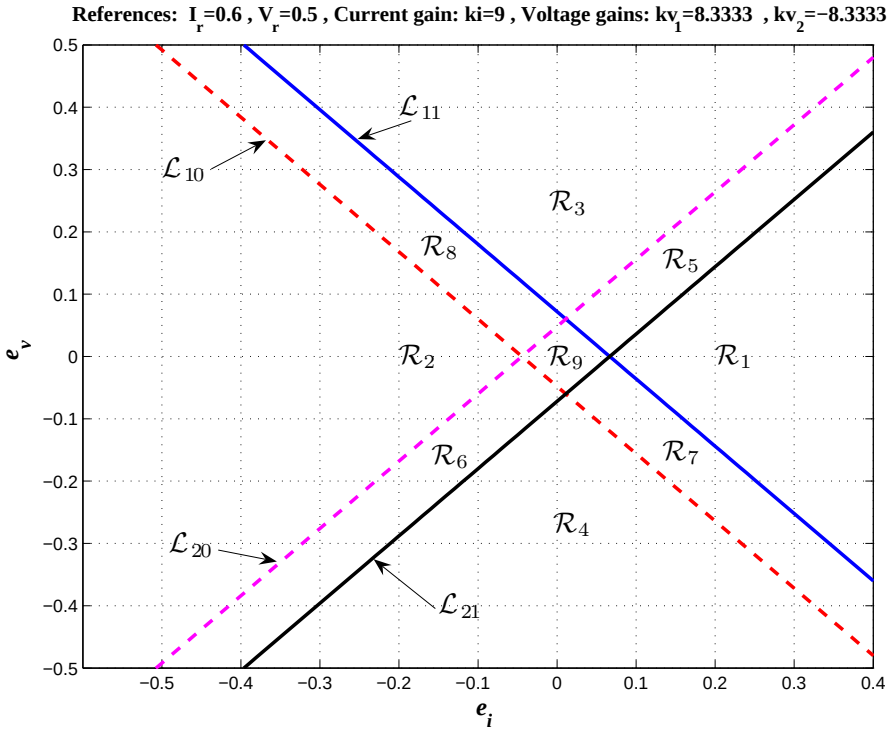

Fig. 12. The error space divided into nine subspaces.

Then $\Delta V < 0$ if $e_i[n] < -\frac{\delta_L}{2}\frac{1-I_r}{1-\delta_L}$. Since $e_i[n] < -\frac{1-I_r}{k_i}$ in region $\mathcal{R}_2$ it is sufficient to choose $k_i < \frac{2(1-\delta_L)}{\delta_L}$ to obtain $\Delta V < 0$. In region $\mathcal{R}_3$ the expression of ΔV is given by:

$$\begin{aligned}\Delta V = &\big(\delta_L(\delta_L-2)+\delta_C^2\big)e_i[n]^2+\delta_L^2 e_v[n]^2+\big(2(1-\delta_L)\delta_L-2\delta_C\big)e_i[n]e_v[n]\\ &+\big(2(1-\delta_L)(V_r-I_r)\delta_L+2I_r\delta_C^2\big)e_i[n]+\big(2\delta_L^2(V_r-I_r)-2\delta_C I_r\big)e_v[n]\\ &+\delta_L^2(V_r-I_r)^2+\delta_C^2 I_r^2\end{aligned} \tag{49}$$

We can check that $\Delta V = 0$ defines a hyperbola in the (e_i, e_v) plane. Since for any initial conditions and reference values in the interval $[0, 1]$ we have $-2 \le e_i[n] \le 2$ and $-2 \le e_v[n] \le 2$ then we can easily verify that region $\mathcal{R}_3$ is located between the hyperbolic branches where $\Delta V < 0$. Similar results can be verified for region $\mathcal{R}_4$. For the other regions, analytic verification gets more tedious in general cases, thus they will not be included. Nonetheless, numerical simulations sketched in Fig.13 delineate that $\Delta V < 0$ in each corresponding region, indeed. Therefore, region $\mathcal{R}$ is an invariant set. In Fig.13, green color stands for negative ΔV and red color for positive ΔV; the color gradually gets lighter when ΔV approaches zero. Notice that regions $\mathcal{R}_5$ to $\mathcal{R}_9$ are situated between the boundary lines where duty cycles are partially or totally not saturated. Now, let $B_r(0)$ be a ball of radius r around the origin such that $B_r(0) \in \mathcal{R}_9$. Moreover, we define $\epsilon > 0$ such that

$$\epsilon = \min_{(e_i[n],e_v[n])\in\mathcal{R}\setminus B_r(0)} |\Delta V| \tag{50}$$

Thus $\Delta V \le -\epsilon$ for all $(e_i[n], e_v[n]) \in \mathcal{R} \setminus B_r(0)$, that is $V(e[n+1]) \le V(e[n]) - \epsilon$ and hence $V(e[n+1]) \le V(e[0]) - m\epsilon$ for some number $m \in \mathbb{N}$. We deduce that the sequence of points $(e_i[n], e_v[n])$ can only stay in $\mathcal{R} \setminus B_r(0)$ for a finite number of periods since $V(e[n]) > 0$ for all n. Besides, since $\mathcal{R}$ is an invariant set, then the sequence $(e_i[n], e_v[n])$ has to enter $B_r(0)$. Eventually, the exponential stability is deduced from the analysis presented in the previous section which in fact concerns $\mathcal{R}_9$.

Figure 14 shows the behavior of the system for each point in the error space. In red circles, we represent the error evolution corresponding to the simulations shown in Fig. 10.

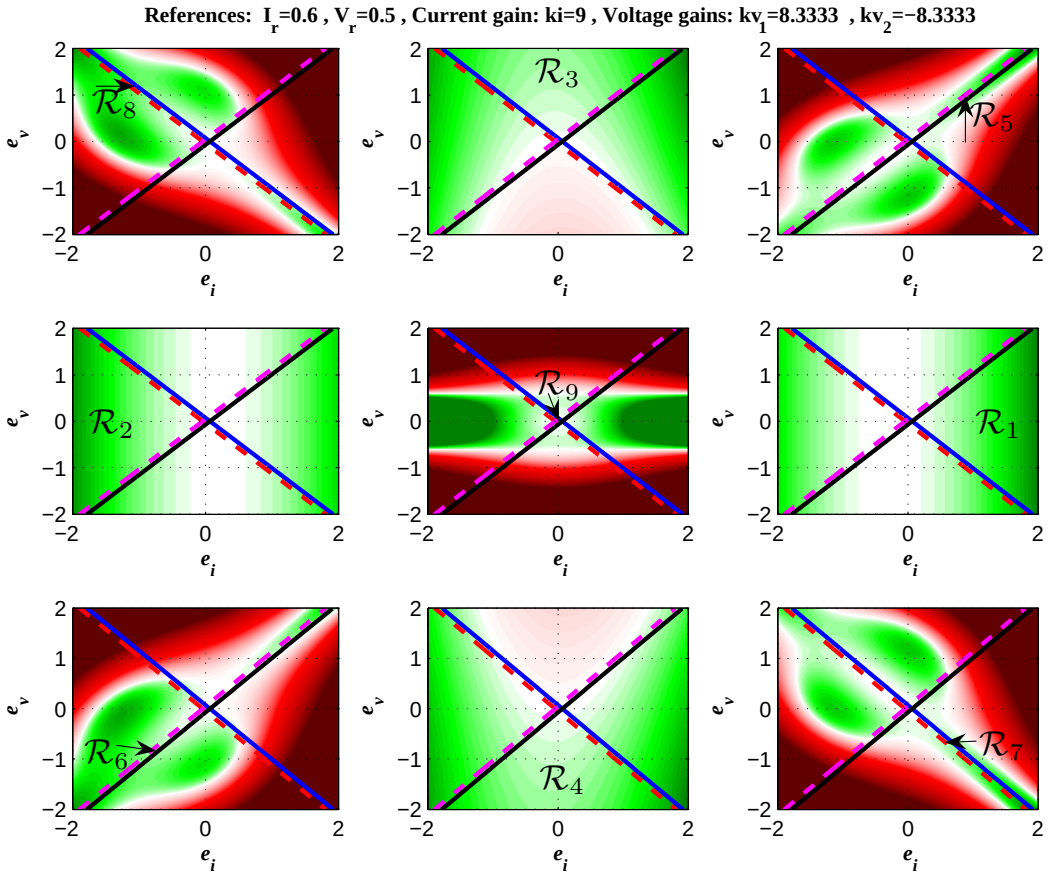

Fig. 13. The color coded values of ΔV corresponding to each model $\mathcal{M}_j$. Green color stands for negative ΔV and red color for positive ΔV; the color gradually gets lighter when ΔV approaches zero.

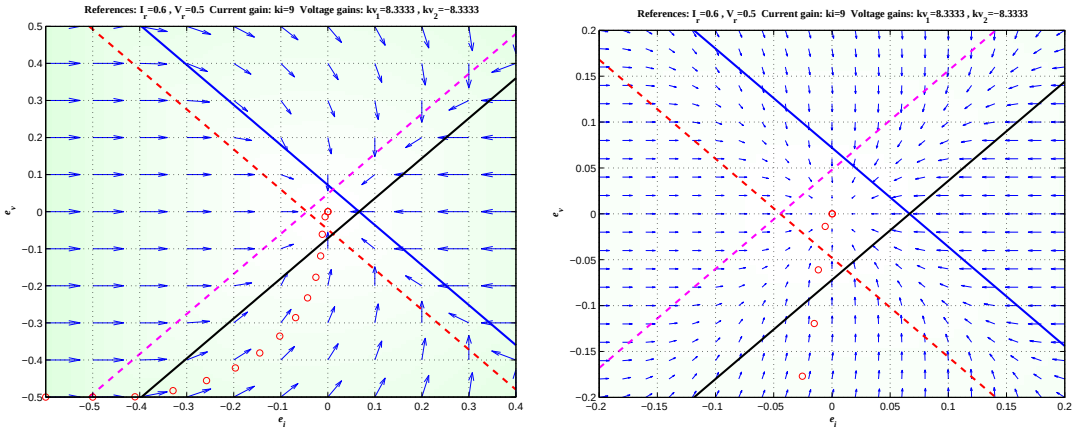

(a) (b)

Fig. 14. (a) The behavior of the error when $k_i = 9$ and $k_{v1} = -k_{v2} = 50/6$, (b) a zoom on the behavior in the neighborhood of the origin.

6. Conclusion

In this paper, we have proposed a simple controller to achieve zero static current and voltage errors for a two-cell DC-DC converter. This method has been proposed after carrying out a nonlinear analysis of the traditional proportional controller in which by increasing the current gain to decrease the current error

sub-harmonic oscillations and chaotic behavior take place. The controller proposed herein, outperforms the traditional controllers in terms of its response speed by appropriately choosing the feedback gain in terms of system parameters. In practice this can be achieved by adopting an adaptive control scheme in which the feedback gains can be updated cycle by cycle in terms of the system state variables. Moreover, we have provided a complete stability analysis where the duty cycle saturation has been taken into consideration. Further work will deal with the implementation of this control scheme as well as its application to other more complex multi-cell converters. Actually, the extension to multi-cell converters may seem straight forward, by adding new terms with different voltage gains to stabilize other flying capacitor voltages. However, further analysis to establish parameter ranges leading to stable behavior is necessary. Moreover, proving the stability in presence of saturating duty cycles seems a challenging task.

Acknowledgment

This work is prepared within a Tunisian-Spanish cooperation framework, under grant A/6828/06 and A/021698/08 and it was partially supported by the Spanish Ministerio de Educación e Innovación under grant TEC-2007-67988-C02-02

References

Bai, X.-M., Li, H.-M., Yang & X.-S. [2006] "Some results on cascade discrete-time systems," *Discrete Dynamics in Nature and Society* (DOI 10.1155/DDNS/2006/14631), 1–8.

Banerjee, S. & Verghese, G. [2001] "Nonlinear phenomena in power electronics: Attractors, bifurcations, chaos and nonlinear control," IEEE Press, New York.

Banerjee S. & Grebogi C. [1999] "Border collision bifurcations in two-dimensional piecewise smooth maps," *Phys. Rev. E* , 59(4), 4052–4061

Deane, J.H.B. & Hamill, D.C. [1992] "Instability, subharmonics and chaos in power electronic systems," *IEEE Trans. Power Elect.* 5(3), 260–268.

di Bernardo, M. & Tse, C. K [2002] "Chaos in power electronics: An overview," in: Chen, G., Ueta, T. (Eds.), Chaos in circuits and systems. (11) World Scientific, New York, Ch. 16, 317–340.

El Aroudi, A., Debbat, M., Olivar, G., Benadero, L., Toribio, E., & Giral, R. [2005], "Bifurcations in DC-DC Switching Converters, Review of Methods and Applications," *Int. J. Bifurcations & Chaos* 15(5), 1549–1578.

El Aroudi, A., Robert, B., Cid-Pastor & A., Martínez-Salamero, L. [2008] "Modelling and Design Rules of a Two-Cell Buck Converter Under a Digital PWM Controller," *IEEE Transactions on Power Electronics*, 23(2), 859–870.

El Aroudi A, Angulo F., Robert B. G. M, Olivar G., & Feki M. [2009] "Stabilizing a Two-Cell DC-DC Buck Converter by Fixed Point Induced Control" *International Journal of Bifurcation & Chaos*, 19, (6), 2043–2057.

Feki M., El Aroudi A., Robert B.G.M., Derbel N. [2008] "Control of a two-cell dc/dc converter in presence of saturating duty cycle," *European Power Electronics-Power Electronics and Motion Control* EPE-PEMC'08, Poznan, Poland.

Feigin, M. I. [1977] "On the structure of C-bifurcation boundaries of piecewise-continuous systems," *Prikladnaya Matematika i Mechanika,* 42, 820–829.

Fossas, E. Olivar, G. [1996] "Study of Chaos in the Buck converter," *IEEE Trans. Circuits Syst. I*, 43(1), 13–25.

Huang, Y., Tse, C. [2009] "Complex behavior of parallel-connected DC-DC converters from nonlinear viewpoint," in: Kocarev, L., Galias, Z., Lian, S. (Eds.), Intelligent Computing Based on Chaos. Springer, New York.

Meynard, T. A., Fadel, M., Aouda, N. [1997] "Modeling of multilevel converters" *IEEE Trans. Ind. Electronics* 44 (3), 356–364.

Nagy, I. [2000] "Nonlinear dynamics in power electronics," in: *Proc. Electrical drives and power Electronics Conf.* pp. 1–15.

Nusse, H. E. [1994] "Border-Collision Bifurcations For Piecewise Smooth One-Dimensional Maps," *International Journal of Bifurcaion and Chaos,* 5-1 pp.189–207.

di Bernardo M., Feigin M.I., Hogan S.J. and Homer M.E. [1999] "Local analysis of c-bifurcations in n-dimensional piecewise-smooth dynamical systems," *Chaos Solitons and Fractals*, 10 (11), pp. 1881–1908.

Pirog, S. Baszynski, M. Czekonski, J. Gasiorek, S. Mondzik, A. Penczek, A. Stala, R. [2006], "Multi-cell DC/DC Converter with DSP/CPLD Control. Practical Results," *Power Electronics and Motion Control Conference*, EPE-PEMC 2006. Aug. 30 2006–Sept. 1

Robert, B. and El Aroudi, A. [2006] "Discrete Time Model of a Multi-Cell DC/DC Converter, Non Linear Approach," *Mathematics and Computers in Simulation* 71(4-6), pp–310-319.

Robert, B., Robert, C. [2002] "Border collision bifurcations in a one-dimensional piecewise smooth map for a pwm current-programmed H-bridge inverter," *International Journal of Control*, 75, 1356–1367.

Tolbert, L. M., Peng, F. Z., [2000] "Multilevel converters as a utility interface for renewable energy systems," in: *IEEE Power Engineering Society Summer Meeting*, 1271–1274.

Tse, C., di Bernardo, M. [2002] "Complex behavior in switching power converters," *Proceedings of the IEEE*, 90 (5), 768–780.

Tse, C.K. [1994] "Chaos from a Buck Switching Regulator Operating in Discontinuous Mode," *Int. J. Circuit Th. Appls.* (4), 263–278.

Wang, X., Zhang, B. Diangong & Jishu Xuebao [2009] "Study of bifurcation and chaos in single-phase SPWM inverter," *Transactions of China Electrotechnical Society* 24(1), 101–107.

Yousefzadeh V., Alarcn E., Maksimovic D [2005] "Three-Level Buck Converter for Envelope Tracking in RF Power Amplifiers," APEC'05- *IEEE Applied Power Electronics Conference*, Austin, Texas.

Zhusubaliyev, Z. T., Soukhoterin E. A., Mosekilde E. [2001] "Border collision bifurcations and chaotic oscillations in a piecewise smooth dynamical system," *Int. J. Bifurcation & Chaos* 11(12), pp. 152–163.

Zhusubaliyev, Z. T., Soukhoterin E. A. and Mosekilde E. [2006] "Birth of bilayered torus and torus breakdown in a piecewise-smooth dynamical system," *Physics Letters A*, 351(3), 167–174.